An Acrylate-Polymer-Based Electrolyte Membrane for Alkaline Fuel Cell Applications

Yanting Luo,[a] Juchen Guo,[a] Chunsheng Wang,*[a] and Deryn Chu[b]

Alkaline fuel cells (AFCs) recently attracted renewed attention because of their potential to surpass proton exchange membrane fuel cells (PEMFCs). The long-existing issues of PEMFCs, including expensive noble-metal catalysts and polymer electrolytes,[1] as well as CO poisoning and inferior temperature endurance,[1,2] prevented them from being used in a broad range of applications.[3] Contrarily, advantages of AFCs include fast kinetics in the reduction of the oxidizing agent[4] and the possibility to use base-metal catalysts.[5] However, a critical challenge for conventional AFCs is the use of aqueous alkaline electrolytes, which can react with CO_2 from air to form carbonate salts (e.g., K_2CO_3). As a result, the performance of the fuel cell would quickly deteriorate. To solve this problem, recent investigations focused on intrinsically OH^--conducting alkaline polymer electrolyte (APE) materials to replace the alkaline electrolytes. By using APEs, the formation of carbonate salts can be prevented, which is attributable to the absence of metal ions. However, carbonate ions might still be formed through a reaction with CO_2, which would result in a reduced OH^- conductivity.[5–7] Application of APEs can also enable a compact design[8] and eliminate corrosion from alkaline solutions. These advantages confirm that APE fuel cells (APEFCs) present a very promising energy conversion technology. Because APEs are a key component determining the ultimate performance, they should exhibit a high OH^- conductivity and superior mechanical properties, and in addition be of low cost.[9]

To date, the most common synthesis route for APEs is chloromethylation of polymers having a phenyl structured backbone, which is followed by quaternization. Many polymers have been used as precursors to synthesize APEs, including polysulfone,[10–12] poly(arylene ether sulfone),[13] polyetherketone,[14] poly(ether imide),[15] polyethersulfone cardo,[16] poly(phthalazinon ether sulfone ketone),[17] poly(dimethyl phenylene oxide),[18] and poly(phenylene).[19,20] Also, a recent study by Lin and co-workers[21] reported high conductivity and mechanical strength for an alkaline polymer electrolyte based on a cross-linked ionic liquid. The phenyl backbones of the polymers have in common that they are all excellent engineering polymers exhibiting good mechanical properties because of rigid ring structures. However, this advantage can be seriously weakened by the chloromethylation–quaternization process, which converts the polymer from an ionic insulator into an ionomer and thus, from hydrophobic to hydrophilic. As a result of the hydrophilicity, the mechanical properties of the APEs in the humid working environment of a fuel cell can be very different from that of the precursors. Because their backbones consist of aromatic groups, these precursor polymers can be modified to exhibit extreme hydrophilicity through the chloromethylation–quaternization process. The resulting APE may have a very high anionic conductivity, but with very poor mechanical properties in humid environment. Therefore, an obvious shortcoming of the chloromethylation–quaternization process is the difficulty to control the degree of chloromethylation and quaternization precisely,[11] thus making it difficult to balance conductivity and mechanical properties. Cost is also a concern, since the aforementioned APE precursors are high-cost polymers because of the sophisticated synthesis process.[22]

In a previous study, we reported a novel APE made from poly (methyl methacrylate-co-butyl acrylate-co-vinylbenzyl chloride) (PMBV).[7] This copolymer was synthesized using solution-free radical polymerization. Xu and co-workers also reported an independent study on APE made from a copolymer using similar polymerization methods.[23] Although this copolymer exhibits a promising performance, our previous study encountered two problems: The three monomers, methyl methacrylate (MMA), butyl acrylate (BA), and 4-vinylbenzyl chloride (VBC), have different reactivity ratios so that they polymerize at different reaction rates. Because of the slow diffusion of propagating copolymer chains and the diluted monomer concentration in the polymerization solution, the monomers with lower reactivity ratios have a smaller possibility for complete conversion. Therefore, the copolymer composition did not match the designed monomer ratio. The second concern is that the molecular weight of the copolymer in our previous study was not as high as expected, which could considerably weaken the mechanical strength. To address these problems, we demonstrate a novel bottom-up synthesis of PMBV by using mini-emulsion polymerization for the first time. Unlike chloromethylation of existing polymers, we synthesized PMBV by using various monomers selected to meet the specifications for conductivity and mechanical strength. Specifically, VBC (15 mol%) contained the chloromethyl functional group, which could be quaternized and then successively ion-exchanged to obtain OH^- conductivity.[24] Polymerized MMA exhibits a high rigidity and toughness. As a result, the MMA monomer (80 mol.%) was chosen to provide mechanical strength. The brittleness inherent to MMA and VBC was overcome by adding a small portion of BA (5 mol%), which conferred flexibility to the resulting APE.

[a] Y. Luo, Dr. J. Guo, Prof. Dr. C. Wang
Chemical and Biomolecular Engineering
2113 Chemical and Nuclear Engineering
University of Maryland, College Park, MD 20742 (USA)
Fax: (+1) 301-314-9126
E-mail: cswang@umd.edu

[b] Dr. D. Chu
Sensors and Electron Device Directorate
US Army Research Laboratory
Adelphi, MD 20783 (USA)

WILEY ONLINE LIBRARY

1

These are not the final page numbers! ↗↗

The mini-emulsion polymerization (see the Supporting Information for mechanism schematics and polymer characterization) is a unique emulsion polymerization technique.[25,26] High shear force (e.g., sonication) is usually employed to disperse monomers in an aqueous phase as droplets. Compared to conventional emulsion techniques, the monomer droplet size is much smaller (a few hundreds of nanometers), and the droplet size distribution is much more uniform. Because of the high surface area of the monomer droplets, all surfactants are adsorbed on the droplet surface to stabilize the dispersion. Moreover, small amounts of an extremely hydrophobic non-active reagent (e.g., hexadecane) dissolved in the monomer droplets are also used as co-stabilizer to further prevent Ostwald ripening. Polymerization is primarily through radical (primary or oligomeric) entry into monomer droplets, when water phase initiator is employed.[27] In mini-emulsions, each monomer droplet can be considered as an individual reactor for bulk polymerization. Because of the small reactor (i.e., droplet) size, the effect of slow diffusion of the propagating chains can be reduced, and high monomer conversions can be achieved. Therefore, the composition of obtained copolymer is in good agreement with the monomer ratio. Also, high molecular weights can be achieved through mini-emulsion polymerization using mild conditions, thus eliminating the difficulties in mixing and heat management in bulk polymerizations.[28] Moreover, water was used as the reaction medium in this mini-emulsion copolymerization, which made it environmentally friendly.

In our experiment, 97% overall monomer conversion was achieved after 120 min reaction (Figure S2 in the Supporting Information). The molecular weight of the obtained PMBV copolymer was 1.5×10^6 g mol^{-1} (Figure S3), which is six times higher than that of the copolymer in our previous study.[7] The composition of the resulting PMBV was 78.8:4.8:16.4 (molar% of MMA/BA/VBC) according to calculations based on the ^{1}H NMR spectrum (Figure S4). This composition is in good agreement with the monomer ratio in the reactant mixture (80:5:15). The glass transition temperature (T_g) of the PMBV copolymer was 102 °C as determined by using differential scanning calorimetry (DSC, Figure S5), which is in agreement with results calculated from measurements performed at 93 °C and based on the composition.[29]

The complete synthesis route for the APE (see the Supporting Information for details of membrane preparation and characterization) is shown in Scheme 1. Firstly, the PMBV copolymer was synthesized by using mini-emulsion polymerization. This was followed by quaternization of PMBV by reaction with trimethylamine (Me₃N) in dimethylformamide (DMF). The quaternized PMBV (QPMBV) was then cast to obtain a membrane and soaked in 6 M KOH at room temperature for 24 h to exchange Cl⁻ with OH⁻. After ion-exchange, the polymer membrane was washed with abundant water until pH 7 was reached. The final product, QPMBV-APE, was obtained after drying was completed. Elemental analysis revealed complete quaternization (all VBC groups were quaternized). The products for each synthesis step are shown in Figure 1. Acid-based back-titration measurements[30] indicated an ion-exchange ca-
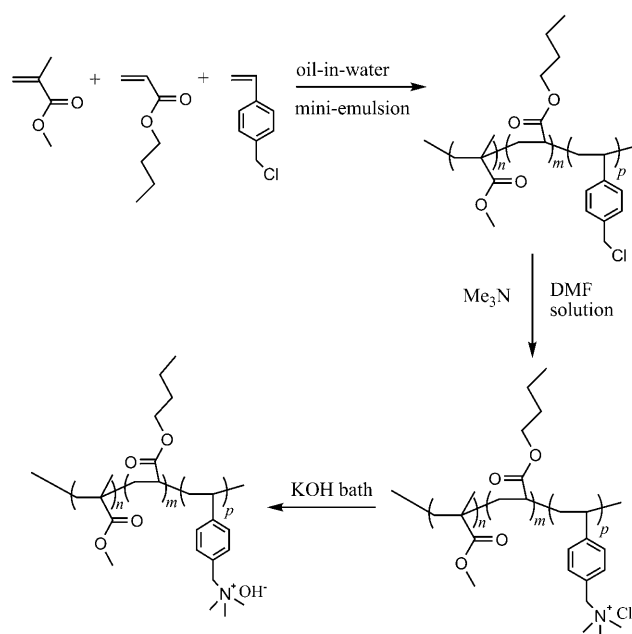
Scheme 1. Synthesis of QPMBV-APE: mini-emulsion copolymerization (initiator: K₂S₂O₈, surfactant: sodium dodecyl sulfate, co-stabilizer: hexadecane), APE quaternization, and ion-exchange.

pacity (IEC) of 1.28 mmol g^{-1}, and the efficiency of ion-exchange was estimated to be approximately 90% (see the Supporting Information). The nature of conducting ions in QPMBV-APE was identified by using a titration method (Figure S8). The titration results indicated that most of the conducting ions (OH⁻) were converted to HCO₃⁻ and/or CO₃²⁻ approximately 60 min after QPMBV-APE was neutralized. The stability of the conductivity at high pH values was also tested in a 6 M KOH solution (Figure S9). The stability test indicated a 3.3% decrease in the IEC of QPMBV-APE being soaked in 6 M KOH solution for 7 days.

Both water uptake and anionic conductivity of the QPMBV electrolyte membranes were measured under fuel-cell opera-
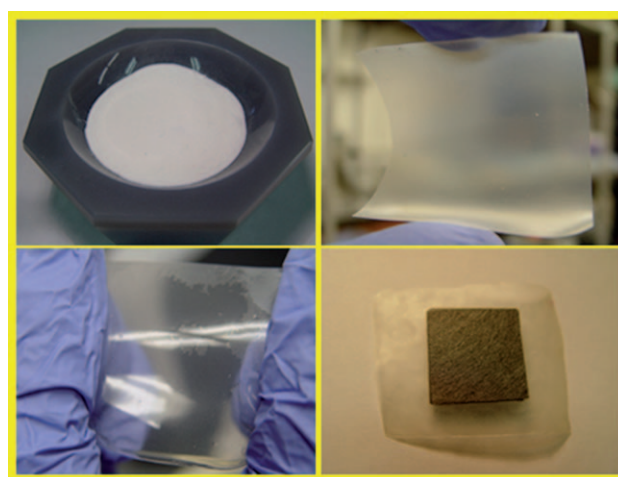
Figure 1. a) PMBV copolymer powder after mini-emulsion copolymerisation; b) QPMBV membrane before ion-exchange being bent; c) ion-exchanged QPMBV-APE membrane being stretched; and d) MEA with QPMBV-APE membrane.

tion conditions [80% relative humidity (RH) and 40–70 °C]. Figure 2 depicts the water uptake of the QPMBV-APE membrane at 80% RH as a function of temperature. The results are based on triplicate measurements. The water uptake at 80% RH was between 20 and 30 wt% in the temperature range from 40 to 70 °C.

The anionic conductivity of QPMBV-APE was measured in a four-probe testing cell (BekkTech, BT-112) by using electrochemical impedance spectroscopy (EIS, Figure S7). Figure 3 shows the development of the conductivities in a temperature range from 50 to 80 °C and at 80% RH. The calculated activation energy was 52.2 kJ mol^{-1}. The high anionic conductivity of QPMBV-APE of up to 43 mS cm^{-1} could be attributed to 15 mol% anions attached to the VBC group in the copolymer.

Prior to performance tests of fuel cells using APE (APE-FC), a membrane electrode assembly (MEA) was fabricated following the standard procedure detailed in the experimental section[31] by using a 50 μm thick QPMBV-APE membrane as electrolyte
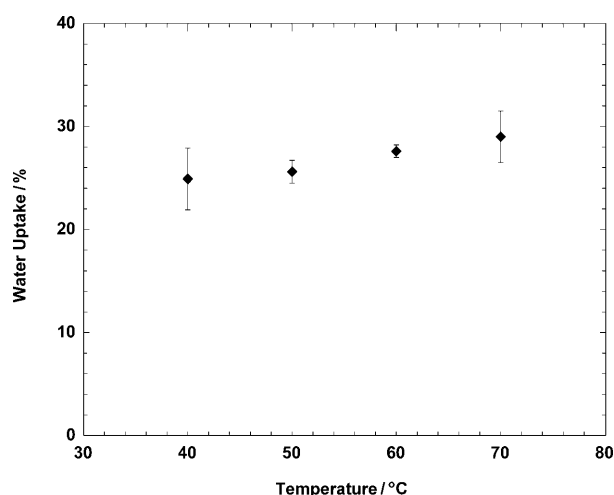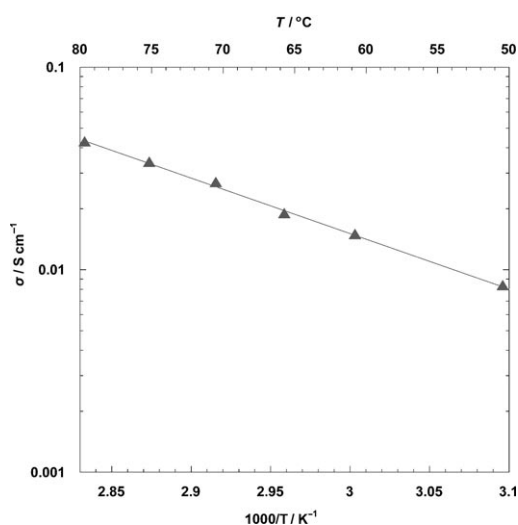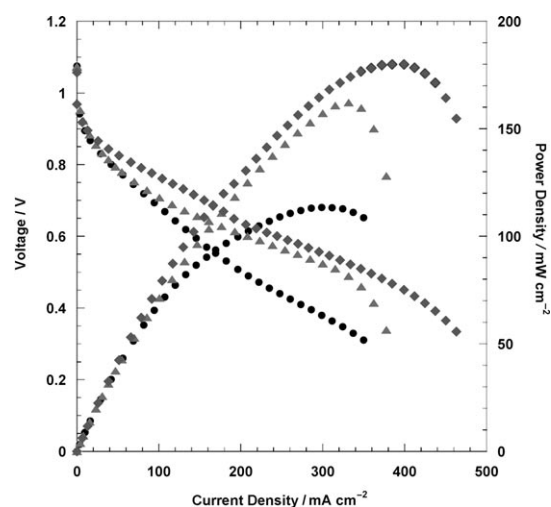
and QPMBV in an ethanol/water solution as ionomer. Pt was used as a catalyst using a loading of 0.4 mg cm^{-2}. Hydrogen and oxygen were used as the fuel and oxidant, respectively, at 100 ± 2 sccm (standard cm^3 min^{-1}). The performance of the QPMBV-APE fuel cells was tested at 80% relative humidity (RH) at various temperatures by using a current scan rate of 3 mA s^{-1} and a back pressure of 10^5 Pa. The use of a low-current scan rate was to ensure that the fuel cell performance reached steady state. As shown in Figure 4, the initial voltage drop ($\approx$100 mV) was mainly attributable to an activation loss of the interfacial electrochemical charge-transfer reaction in the catalyst layer of the MEA.[32] After the initial activation loss, the fuel cell voltage deceased gradually with an increase in current density. The fuel-cell performance was improved when the temperature increased from 50 to 70 °C. At 70 °C, the current density reached 500 mA cm^{-2}, and the fuel cell could deliver a peak power density of 180 mW cm^{-2}. Even at lower temperatures (60 °C and 50 °C), the fuel-cell performance using QPMBV-APE had maximum power densities of 160 and 115 mW cm^{-2}, respectively. This is among the best performances reported for APE membranes.[20,33–36] The energy output was approximately four times higher than in our previous study.[7] This improvement can be attributed to the fivefold increased anionic conductivity and the twofold thinner membrane used. Although the Pt catalyst loading was smaller, these improvements give rise to a better performance.

In conclusion, a novel APE was synthesized through mini-emulsion copolymerization with designed hydrophobic and hydrophilic (anion conducting) segments to balance conductivity with mechanical strength. Our results indicated that the intentionally incorporated VBC functional groups were almost completely quaternized and ion-exchanged. The exceptional APE-FC performance revealed the great potential of QPMBV-APE. Not only was a promising APE synthesized, but this study also demonstrated a novel concept: alkaline polymer electrolytes can be designed bottom-up through mini-emulsion polymerization by precisely selecting the functional monomers.

Figure 2. Water uptake by the OH$^-$-exchanged QPMBV-APE membrane as a function of temperature at 80% RH.

Figure 3. Conductivity of the QPMBV-APE membrane as a function of temperature at 80% RH.

Figure 4. I–V polarization curves of the QPMBV-APE-FC at 80% RH (● 50 °C; ▲ 60 °C; ◆ 70 °C).

These are not the final page numbers! ↗↗

The conductivity and mechanical durability of the APE can be tailored by selecting desirable monomer and controlling the polymerization process. In this way, both properties can be improved without compromising the other. Furthermore, the mini-emulsion copolymerization process can be used to synthesize high molecular weight APEs with superior mechanical properties. Control of the polymerization process, such as step-wise monomer feeding, can be used to introduce favorable polymer chain sequences that could lead to hydrophobic and hydrophilic micro-phase separation. This will the subject of future studies.

Experimental Section

Mini-emulsion copolymerization

The mini-emulsion was prepared by dispersing a mixture of monomers (30 g) with a designed molar ratio (MMA/BA/VBC = 80:5:15) and hexadecane (0.12 g) in an aqueous sodium dodecyl sulfate solution (SDS, 0.01 mol L^{-1}, 150 mL) by applying ultrasonic shearing to form a stable mini-emulsion using a homogenizer (Omni Sonic Ruptor 400) at 30% power output for 9 min. The polymerization was initiated by injection of the initiator potassium peroxydisulfate (KPS) (0.01 mol L^{-1} in the water phase) into the mini-emulsion at 70 °C under a nitrogen atmosphere. The reaction was terminated after 4 h by quenching in an ice bath. The copolymer was filtered and dried in a fume hood overnight and was further dried in a vacuum oven at 60 °C for 24 h.

Membrane preparation

The obtained PMBV was dissolved in dimethylformamide (DMF) at 80 °C and quaternized using trimethylamine (Me$_3$N, Sigma–Aldrich) at 80 °C for 2 h by bubbling Me$_3$N into the solution while stirring. The QPMBV solution in DMF was then cast as a film and dried in a vacuum oven at 60 °C for 24 h. The obtained membrane was soaked in a 6 M KOH solution overnight to exchange Cl$^-$ with OH$^-$. The OH$^-$-exchanged membrane was washed with deionized water until pH 7 was reached.

Fabrication of the membrane electrode assembly (MEA)

Carbon paper (Toray, TGP-H-60) was first brushed by using a PTFE/carbon black slurry ((35/65 wt%, 0.2 ± 0.02 mg cm^{-2}). The Pt/C catalyst (60/40 wt%) was dispersed in a dilute OH$^-$-exchanged QPMBV solution in an ethanol/water mixture (50/50 vol%) by sonication. This catalyst dispersion was sprayed onto the processed carbon paper giving a Pt loading of 0.4 ± 0.05 mg cm^{-2}. Then the QPMBV-APE membrane was sandwiched between two catalyst-loaded carbon papers (5 cm^2) by using a hot-press (Carver 973214 A) under a pressure of 2×10^5 Pa at 60 °C for 10 min to obtain the MEA for the performance test.

Acknowledgements

[1] R. Devanathan, *Energy. Environ. Sci.* **2008**, *1*, 101–119.
[2] J. J. Baschuk, X. Li, *Int. J. Energy Res.* **2001**, *25*, 695–713.
[3] S. J. Hamrock, M. A. Yandrasits, *Polym. Rev.* **2006**, *46*, 219–244.
[4] B. Y. S. Lin, D. W. Kirk, S. J. Thorpe, *J. Power Sources* **2006**, *161*, 474–483.
[5] H. Yanagi, K. Fukuta, *ECS Trans.* **2008**, *16*, 257–262.
[6] A. Filpi, M. Boccia, H. A. Gasteiger, *ECS Trans.* **2008**, *16*, 1835–1845.
[7] Y. Luo, J. Guo, C. Wang, D. Chu, *J. Power Sources* **2010**, *195*, 3765–3771.
[8] J. R. Varcoe, R. C. T. Slade, *Fuel Cells* **2005**, *5*, 187–200.
[9] D. Tang, J. Pan, S. Lu, L. Zhuang, J. Lu, *Sci. China: Chem.* **2010**, *53*, 357–364.
[10] J. Pan, S. Lu, Y. Li, A. Huang, L. Zhang, J. Lu, *Adv. Funct. Mater.* **2010**, *20*, 312–319.
[11] G. Wang, Y. Weng, D. Chu, R. Chen, D. Xie, *J. Membr. Sci.* **2009**, *332*, 63–68.
[12] S. Lu, J. Pan, A. Huang, L. Zhuang, J. Lu, *Proc. Natl. Acad. Sci. USA* **2008**, *105*, 20611–20614.
[13] J. Zhou, M. Unlu, J. A. Vega, P. A. Kohl, *J. Power Sources* **2009**, *190*, 285–292.
[14] Y. Xiong, Q. Liu, Q. Zeng, *J. Power Sources* **2009**, *193*, 541–546.
[15] G. Wang, Y. Weng, J. Zhao, R. Chen, D. Xie, *J. Appl. Polym. Sci.* **2009**, *112*, 721–727.
[16] L. Li, Y, Wang, *J. Membr. Sci.* **2005**, *262*, 1–4.
[17] J. Fang, P. Shen, *J. Membr. Sci.* **2006**, *285*, 317–322.
[18] L. Wu, T. Xu, D. Wu, X. Zheng, *J. Membr. Sci.* **2008**, *310*, 577–585.
[19] M. R. Hibbs, C. H. Fujimoto, C. J. Cornelius, *Macromolecules* **2009**, *42*, 8316–8321.
[20] E. E. Switzer, T. S. Olson, A. K. Datye, P. Atanassov, M. R. Hibbs, C. Fujimoto, C. J. Cornelius, *Electrochim. Acta* **2010**, *55*, 3404–3408.
[21] B. Lin, L. Qiu, J. Lu, F. Yan, *Chem. Mater.* **2010**, *22*, 6718–6725.
[22] K. Cousins, *Polymers for Electronic Components*, Rapra Technology, UK, **2001**, p. 15.
[23] H. Xu, J. Fang, M. Guo, X. Lu, X. Wei, S. Tu, *J. Membr. Sci.* **2010**, *354*, 206–211.
[24] L. Dominguez, J. Economy, K. Benak, C. L. Mangun, *Polym. Adv. Technol.* **2003**, *14*, 632–633.
[25] J. Reimers, F. J. Schork, *J. Appl. Polym. Sci.* **1996**, *59*, 1833–1841.
[26] F. J. Schork, J. Guo, *Macromol. React. Eng.* **2008**, *2*, 287–303.
[27] J. Guo, F. J. Schork, *Macromol. React. Eng.* **2008**, *2*, 265–276.
[28] Y. Luo, I. Chou, W. Chiu, C. Lee, *J. Polym. Sci., Part A: Polym. Chem.* **2009**, *47*, 4435–4445.
[29] J. E. Mark, A. Eisenberg, W. W. Graessley, *Physical Properties of Polymers*, American Chemical Society, Washington DC, USA, **1993**, p. 87.
[30] G. Hwang, H. Ohya, *J. Membr. Sci.* **1998**, *140*, 195–203.
[31] S. Gamburzev, A. J. Appleby, *J. Power Sources* **2002**, *107*, 5–12.
[32] R. O'Hayre, S.-W. Cha, F. B. Prinz, W. Colella, *Fuel Cell Fundamentals*, John Wiley & Sons, New York, **2005**, pp. 204–224.
[33] E. Agel, J. Bouet, J. F. Fauvarque, *J. Power Sources* **2001**, *101*, 267–274.
[34] K. Matsuoka, Y. Iriyama, T. Abe, M. Matsuoka, Z. Ogumi, *J. Power Sources* **2005**, *150*, 27–31.
[35] J. R. Varcoe, R. C. T. Slade, *Electrochem. Commun.* **2006**, *8*, 839–843.
[36] S. Gu, R. Cai, T. Luo, Z. Chen, M. Sun, Y. Liu, G. He, Y. Yan, *Angew. Chem.* **2009**, *121*, 6621–6624; *Angew. Chem. Int. Ed.* **2009**, *48*, 6499–6502.

↖↖ These are not the final page numbers!

COMMUNICATIONS

Monomers rule: A novel bottom-up synthesis of an alkaline polymer electrolyte by applying mini-emulsion copolymerization is demonstrated. This synthesis approach can be used to control and tune conductivity and mechanical properties of the electrolyte. The processed electrolyte membrane exhibits superior power performance in alkaline fuel cells, which demonstrates the great potential of these membranes to be used in next generation energy conversion systems.
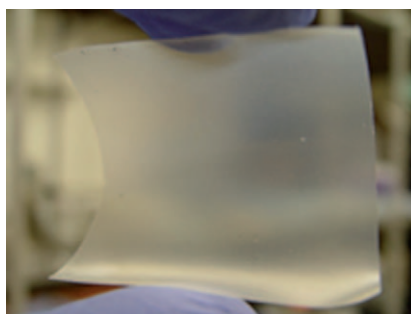
Y. Luo, J. Guo, C. Wang,* D. Chu

■■ – ■■

An Acrylate-Polymer-Based Electrolyte Membrane for Alkaline Fuel Cell Applications 🖳
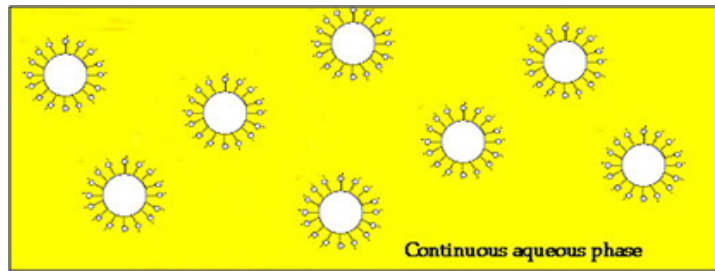
Supporting Information

An Acrylate-Polymer-Based Electrolyte Membrane for Alkaline Fuel Cell Applications

Yanting Luo,[a] Juchen Guo,[a] Chunsheng Wang,*[a] and Deryn Chu[b]

cssc_201100287_sm_miscellaneous_information.pdf

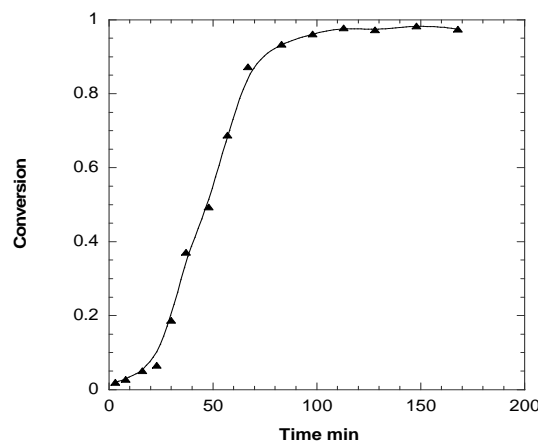## 1. Miniemulsion Copolymerization and Polymer Chracterization

- **Only Monomer Droplets**
- **Droplet Diameter (50-300 nm)**
- **Sonication or Homogenization**
- **Costabilized (hexadecane, cetyl alcohol)**
- **Nucleation in Droplets**
- **No Mass Transfer (except aq. radicals)**

Figure S1. Miniemulsion copolymerization system schematics.

Conversion Test: Prior to the copolymerization, aluminum weight pans pre-loaded with trace amount of hydroquinone (as polymerization terminator) were weighted and recorded. During the copolymerization, small amount of miniemulsion reaction content was drawn from the reactor flusk from various intervals, and put in the aluminum pan and weighted. After completely drying the drawn miniemulsion content in vaccum oven overnight, the obtained residue (with the pan) was weighted again. The monomer conversion was cacluated by gravimetric method using following equation

$$Conversion = \frac{W_{dry} - W_{wet} \times (SDS + KPS + HD)wt\%}{W_{wet} \times \eta} \tag{1}$$

where W_{dry} was the weight of the residue in the weighting plate; $(SDS+KPS+HD)$ $wt\%$ is the total weight percentage of SDS (surfactant), KPS (initiator), and hexadecane (costabilizer) in the reactant mixture; W_{wet} was the weight of the miniemulsion content drawn to the weight pan; and η is the weight percentage of monomers in the entire reactant mixture. Figure S2 is the overall monomer conversion as a function of reaction time. It indicates 97% conversion of the monomers after 120 min.


Figure S2. Miniemulsion copolymerization monomer conversion plot.

Molecular Weight: GPC (gel permeation chromatography, Waters 2410 Refractive Index Detector, Polymer Labs mixed-bed column ranged from 500 to 10,000,000 g/mol) was used to determine the molecular weight of PMBV. Tetrahydrofuran (THF) was used as the carrier solvent in GPC. The flow rate of THF was 1 ml min^{-1}. Five PMMA standard samples (polymer laboratory®) with different

molecular weights (GPC spectra shown in Figure S3a) were used as the standards to obtain a third-order polynomial equation for the calibration curve of molecular weight versus retention time. Figure S3b was the GPC spectrum of the PMBV copolymer. Table S1 listed the GPC results of the PMBV copolymer.

Table S1. MWs of PMBV

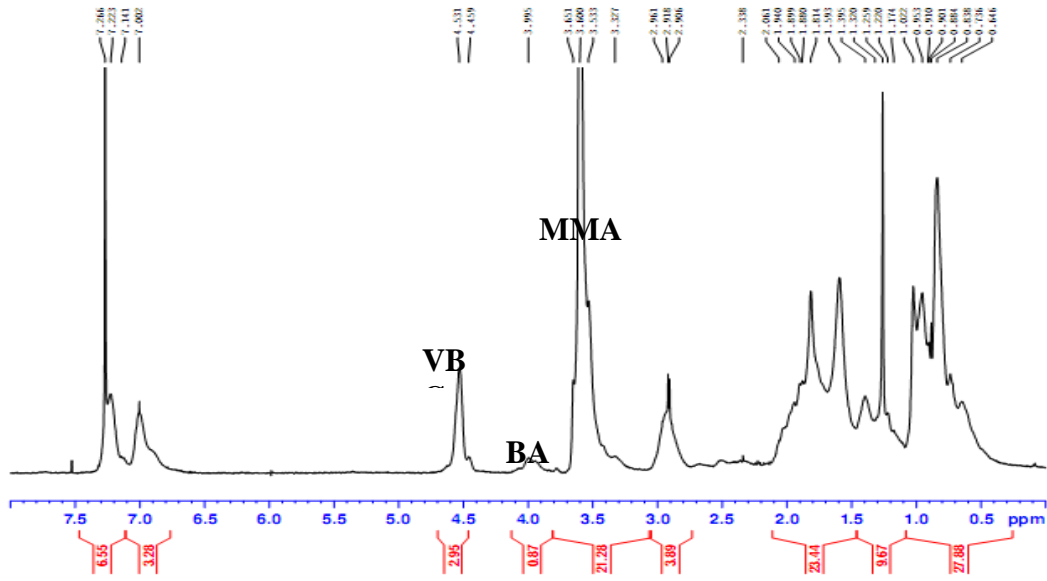|	PMBV
Number-average MW g/mol	6.4×10^5
Weight-average MW g/mol	1.5×10^6
PDI	2.3
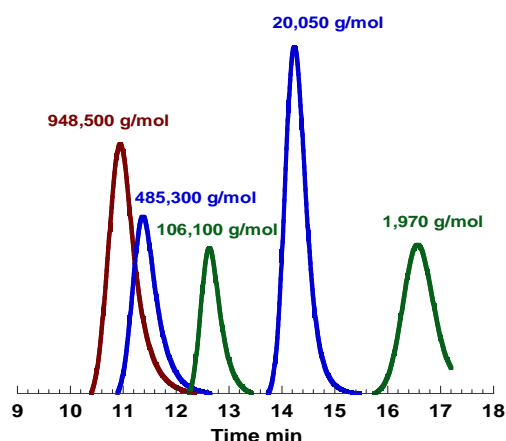
Figure S3. (a) GPC spectra of standard polymer.
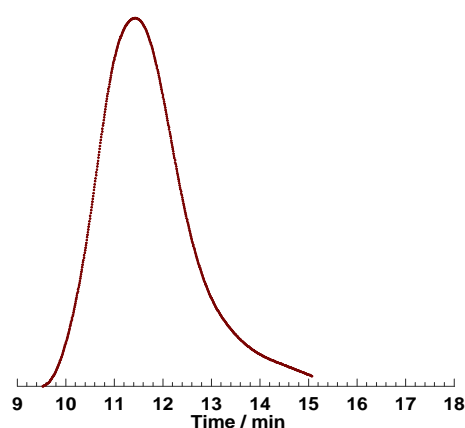
Figure S3. (b) GPC spectrum of PMBV.

Polymer Composition: ^{1}H-NMR (proton nuclear magnetic resonance, Bruker DRX-400 high resolution) spectrum was used to calculate the composition of the obtained PMBV. Figure S4 was the ^{1}H-NMR spectrum of copolymer PMBV. Characteristic peaks of chemical shifts(δppm) at 4.495(d, 2H, -CH$_2$Cl in VBC), 3.995(d, 2H, -OCH$_2$- in BA), and 3.595(t, 3H, -OCH$_3$ in MMA) confirmed PMBV copolymer. The composition was list in Table S2. It was shown that the composition in PMBV caculated from NMR is in great agreement with that of monomers.

Table S2. composition of PMBV

|	MMA	BA	VBC
Composition in PMBV mol.%	78.8	4.8	16.4
Recipe Monomer Ratio mol.%	80	5	15

Figure S4. ^{1}H-NMR spectrum of copolymer PMBV

Glass Transition Temperature: The glass transition temperature (T_g) of PMBV copolymer could be estimated by the following expression

$$\frac{1}{Tg} = \frac{W_{PMMA}}{Tg_{PMMA}} + \frac{W_{PBA}}{Tg_{PBA}} + \frac{W_{PVBC}}{Tg_{PVBC}}$$

(2)

where W with subscript is the mass ratio of each component in the polymer, and T_g with subscript represents the glass transition temperature of the corresponding homopolymer. Table S3 listed the T_g of homopolymers for the PMBV content (Data were obtained from the Polymer Hand Book). The T_g of PMBV was caculated from Equation (2). DSC (Differential scanning calorimetry, TA Instruments Q100) was also used to determine the T_g of PMBV. Figure S5 was the DSC plot of PMBV. The peak of the derivative heat flow versus temprature curve indicated a T_g of 102 ºC. The difference between glass transition temperatures obtained from these two methods is mainly from the rotational barriers between two different monomer pairs.

Table S3. estimated *Tg* in ideal situation for PMBV

	Tg
PMMA (78.8 mol. %)	105
PBA (4.8 mol. %)	-49
PVBC (16.4 mol. %)	114
PMBV	92.9
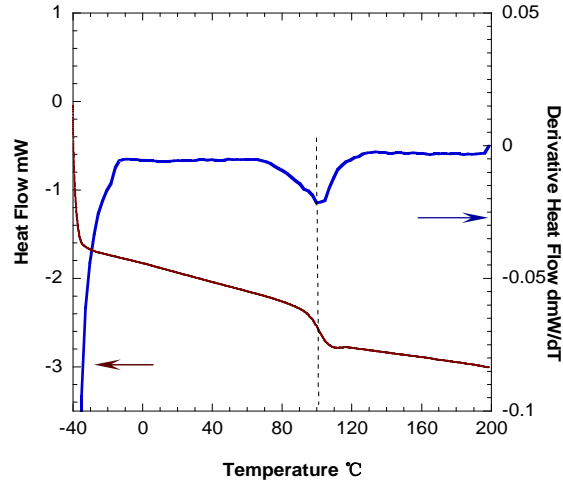
Figure S5. DSC thermo gram of PMBV

2. Electrolyte Membrane Preparation and Characterization

Element Analysis: The degree of quaternization was determined by elemental analysis (Atlantic Microlab® of combustion). Assuming all functional group VBC was reacted with TMA (Me$_3$N), the theoretical composition of N in the QPMBV copolymer can be calculated by

$$W_N = \frac{M_N \times W_{VBC}}{M_{MMA} \times W_{MMA} + M_{BA} \times W_{BA} + (M_{VBC} + M_{Me_3N}) \times W_{VBC}} \times 100\% \tag{3}$$

where M with subscript is the molecular weight of the corresponding monomer, compound, or element; W with subscript is the composition molar ratio of the corresponding substance. Using this formula, the theoretical weight percentage of N element was 2 wt. % in the QPMBV. Combustion test result suggested 2.26 wt. % N in the QPMBV after two hours of quaternization, and did not change afterwards. This value is within the experimental error ($\pm 0.5\%$). The excess amount of N is possibly due to the trace of DMF solvent left in the membrane even after vacuum drying.

Ion Exchange Capacity (IEC) and Ion Exchange Efficiency (IEE): The IEC of APE membrane was measured by acid-based back-titration. The dry membrane sample was immersed in 6M KOH solution overnight to exchange into OH⁻ form. After being washed with de-ion water until pH reaching 7, the sample was soaked in 30mL of 0.01M standardized HCl solution for one day to ensure the neutralization of OH⁻ in the membrane. The IEC value was then determined from back-titration of the excess HCl with 0.01M NaOH solution, which can be calculated by

$$IEC = \frac{(V_{HCl} - V_{NaOH}) \times C}{m_{dry}} (mmol \cdot g^{-1}) \tag{4}$$

where V_{HCl} is the volume of HCl solution for membrane soaking; V_{NaOH} is the volume of NaOH solution used in back-titration; C is the concentration of HCl and NaOH solution in mmol mL⁻¹. m_{dry} is the mass of the dry membrane. The OH⁻ weight percentage of the exchanged cation sites can be calcuated as

$$W_{OH} = IEC \times M_{OH} \times 100\% \tag{5}$$

where M_{OH} is the molecular weight of OH⁻. The calculation showed that the changed OH⁻ weight percentage was 2.2%. That indicated an IEE (Equation 6) of 89.6% for paired cation sites that changed from Cl⁻ to OH⁻ form.

$$IEE = \frac{W_{OH}}{W_N \times \frac{M_{OH}}{M_N}} \tag{6}$$

QPMBV-APE Tensile Test: Tensile test was performed at the stretch rate of 1N/min at room temperature. The tensile test was performed in the worst scenario of fuel cell operation environment, i.e. the QPMBV-APE was fully saturated with DI water by soaking in

DI water for one hour before the test. Water uptake at full water saturation was determined by gravimetric method. The strain vs. stress plot is shown in Figure s6, and the obtained mechanical properties are listed in Table S4. The Young's modulus and elongation indicated an elastic QPMBV-APE membrane.
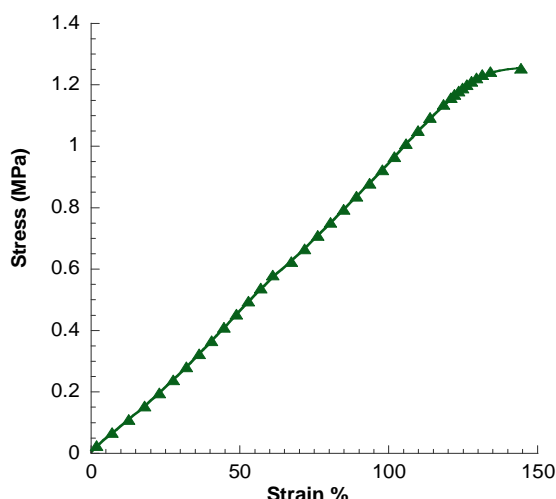
Figure S6. stress-strain plot for water saturated QPMBV-APE.

Table S4. Basic properties of QPMBV-APE

Properties at ambient temperature	QPMBV-APE
Thickness(μm)	50
Young's modulus(MPa) [a]	0.93
Yield Stress(MPa) [a]	1.25
Elongation at yield [a]	130%
Water uptake [a]	325 ± 32 %

[a] saturated with water

Swelling ratios: Three dimemential (length, width, and thickness) swelling ratios were measured in the situation of fully saturated with water at room temperature. The dimential swelling ratios was calculated as:

$$SR = \frac{l_{wet} - l_{dry}}{l_{dry}} \times 100\% \tag{7}$$

The three dimential swelling ratios at room temperatures are listed in Table S5.

Table S5. Swelling ratios at room temperature in fully water saturated situation

	Length	Width	Thickness
Swelling Ratio (%)	31.6	29.0	91.6

Mechanical Stability in Hot Water: Swelling ratios of the membrane in 70 °C water were also measured after full water saturation. The swelling ratios were measured again after 24 hrs soaking in 70 °C water as an indication of the mechanical stability in high temperature water. There was only a slight increase in swelling ratios after 24 hrs as shown in Table S6, which implied that our QPMBV membrane was durable in hot water.

<table>
<tr><td colspan="4" align="center">***Table S6.*** Mechanical stability in hot water</td></tr>
</table>

		70 °C	70 °C after 24hrs
Swelling Ratios (%)	Length	50.6	52.5
	Width	40.3	44.8
	Thickness	125.0	137.5

Conductivity Measurement: Anion conductivities were measured using EIS (electrochemical impedance spectroscopy, Gamry Instruments 3000, Potentiostat/ Galvanostat/ ZRA) with the fixture of conductivity cell (BekkTech, BT-112). The temperature and humidity in the conductivity cell were controlled using the fuel cell test station (Arbin, 2000). The relativive humidity (RH) was adjusted by dew point temperature (DPT) and gas supply temperature (GST) from Arbin test station. Figure S7 showed the Nyquist plot of the QPMBV-APE in different temperatures. The conductivies of QPMBV-APE at different temperatures at 80% RH were calculated using equation 7 and summerized in Table S6.

$$\sigma = \frac{l}{Rab} \tag{8}$$

where *l* is the membrane thickness, *a* is the membrane width, *b* is the membrane length between the probes and *R* is the resistance obtained from EIS.
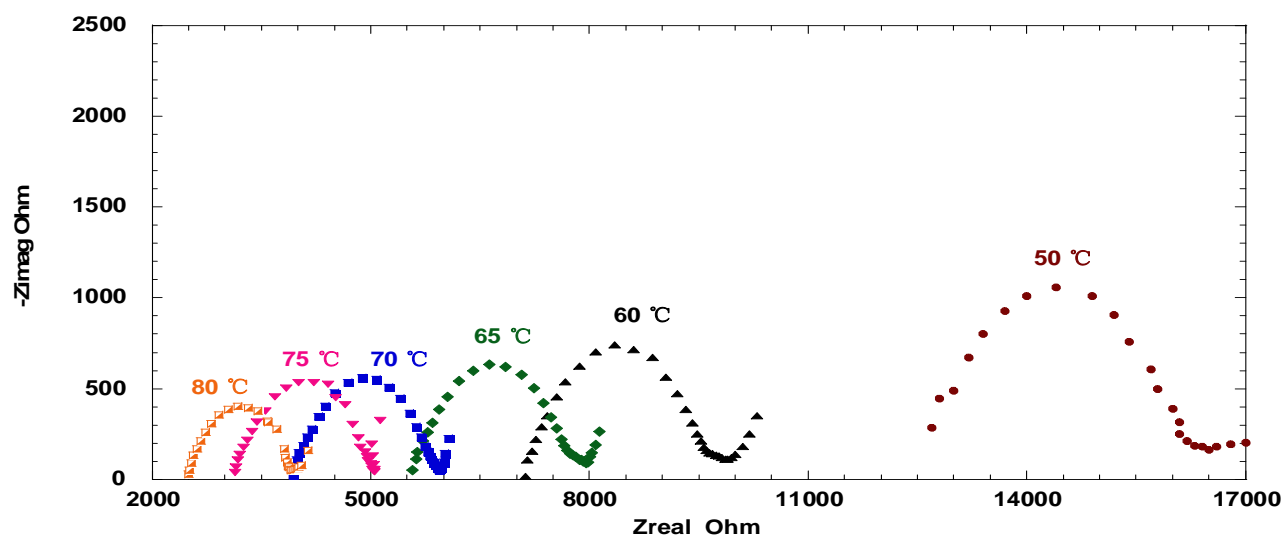
Figure S7. Nyquist plot of APE from 50 ℃ to 80℃

Table S7. Conductivities of QPMBV-APE at different temperatures at 80% RH

T (°C)	50	60	65	70	75	80
Conductivity(S cm^{-1})	0.84×10^{-2}	1.5×10^{-2}	1.9×10^{-2}	2.7×10^{-2}	3.4×10^{-2}	4.3×10^{-2}

Determination of Conducting Ion: Warder titration was used to identify different conducting Ions. The detailed procedure was as follows: The QPMBV memebranes were kept in 6M KOH sultion. Prerior to the tiration, a number of QPMBV membranes were taken out of the KOH solution at the same time, and rinsed with de-ionized (DI) water until the pH of these membranes reached 7. Then, one of these

membranes was put in to 20 mL DI water for the titration, while the rest of them were stored in ambient condition for later titration experiments. Two to three drops of phenolphthalein solution was added into the DI water beaker containing the QPMBV membrane right away, and it was immediately titrated with 0.01M HCl solution till the membrane lost its pink color. The voume of HCl solution being used at thin piont was recorded as V_1. After that, one to two drops of methyl orange solution was added to the same membrane. HCl solution was continuously added till orange color changed to red. The total volume of HCl being used at this point was recorded as V_2. This experiment was repeated around every 10 minutes with a fresh membrane stored in the DI water bath. The IECs attributed to OH$^-$ and CO$_3^{2-}$/HCO$_3^-$ could be calculated by:

$$IEC_{OH^-} = \frac{C_{HCl} \times (2V_2 - V_1)}{m_{dry}}$$

(9)

and

$$IEC_{CO_3^{2-}/HCO_3^-} = \frac{C_{HCl} \times (V_2 - V_1)}{m_{dry}}$$

(10)

where C_{HCl} is the concentration of HCl, and m_{dry} is the weight of the dry membrane.
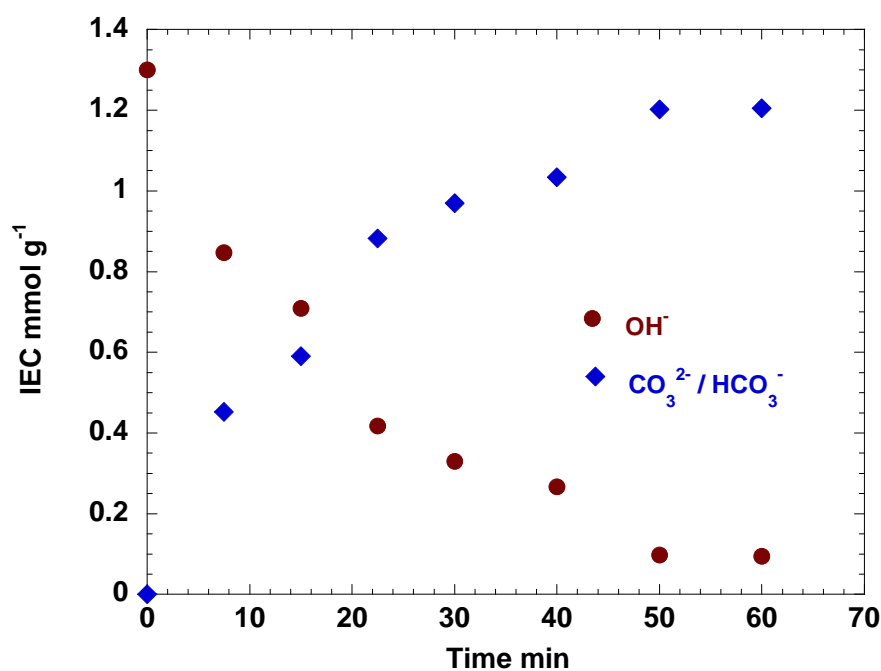
Figure S8. Concentrations of anions in the QPMBV-APE as a function of time.

Chemical Stability in High-pH Environment: we measured the IEC of the QPMBV membrane in 6M KOH solution as a function of time at room temperature. The membranes were kept in 6M KOH solution at room temperature. For the IEC measurement, one membrane was taken out of the KOH solution after each interval, and washed by DI water to pH 7. The IEC of the washed membrane was then determined by acid-based back-titration, as described in IEC and IEE measurement section. As shown in the following plot, our stability test showed a slight 3.3 % decrease of IEC after 7 days in 6M KOH solution.
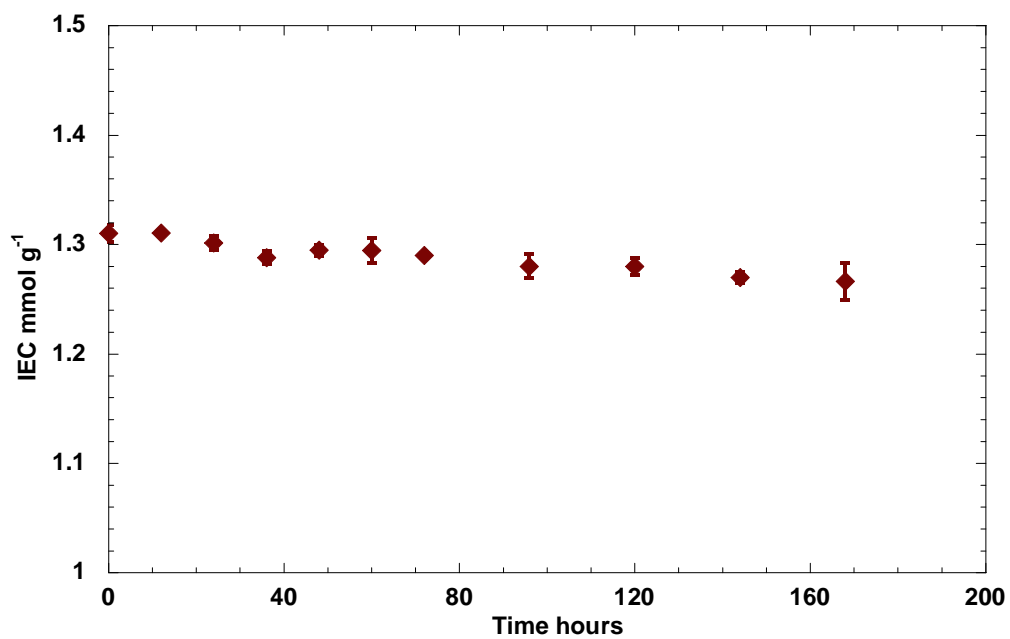
Figure S9. Ion exchange capacity of the QPMBV-APE as a function of time in 6M KOH solution.